


Effects of enzymolysis and fermentation on the antioxidant activity and functional components of a coarse cereal compound powder based on principal component analysis and microstructure study

Yue Chen  | Lan Chen | Zhigang Xiao | Lu Gao 

College of Grain, Shenyang Normal University, Shenyang, Liaoning, China

Correspondence

Lu Gao, Shenyang Normal University, 253 Huanghe North Street, Shenyang, Liaoning 110034, China.
Email: elegancegaolu@126.com

Funding information

Special Fund of Liaoning Provincial Universities' Fundamental Scientific Research Projects, Grant/Award Number: LJKZ0998

Abstract: In this study, a coarse cereal compound powder (CCCP) was prepared through enzymolysis, fermentation, and joint treatment with 10 coarse cereal types as raw materials. Using 10 evaluation indices, namely the scavenging capacity of 1,1-diphenyl-2-picrylhydrazyl (DPPH•), 2,2'-azino-bis-(3-ethylbenzthiazoline-6-sulfonic acid) (ABTS⁺), hydroxyl (OH•) and superoxide anion (O₂⁻), the Fe²⁺ chelating capacity, the content of anthocyanin, flavone, soluble dietary fiber, reducing sugar and protein, antioxidant activity, and functional components of CCCP prepared by different methods were compared. Principal component analysis (PCA) was performed to establish a quality evaluation model of CCCP. Then, the effects of different treatments on the microstructure of CCCP were investigated. Two principal components (PCs) were extracted from PCA, with a cumulative contribution rate of 97.014%. In addition, the analysis of thermodynamic properties indicated that the initial gelatinization temperature of CCCP decreased after enzymolysis and fermentation and that it was easier to gelatinize. Particle size analyses revealed that different treatments could reduce the sample particles to different degrees. The average particle size in the three study groups decreased. Scanning electron microscopy (SEM) revealed that after different treatments, the samples were destroyed to different extents, which facilitated easy dissolution of active substances. Fourier-transformed-infrared spectroscopy (FTIR) revealed that the changes of CCCP functional groups after fermentation and joint treatment were more significant than those after enzymolysis.

KEYWORDS

coarse cereal compound powder, enzymolysis, fermentation, microstructure, principal component analysis

This is an open access article under the terms of the [Creative Commons Attribution-NonCommercial](https://creativecommons.org/licenses/by-nc/4.0/) License, which permits use, distribution and reproduction in any medium, provided the original work is properly cited and is not used for commercial purposes.

© 2022 The Authors. *Journal of Food Science* published by Wiley Periodicals LLC on behalf of Institute of Food Technologists.

Practical Application: In this study, enzymolysis and fermentation techniques were used to improve the antioxidant activity and functional components of CCCP, and the effects of different treatments on the microstructure of CCCP were investigated. The bioavailability and nutrient composition of CCCP could be significantly improved by pretreatment, provide useful reference for the development of beneficial ingredients in cereal meal products and the application of different pretreatment methods.

1 | INTRODUCTION

Compound powder is a type of powdered product that is prepared using various raw materials in a particular proportion. The processing method of this product is simple, and such product is highly portable. Coarse cereals are rich in various nutrients and bioactive components. The antioxidant activity and functional components of CCCP can be improved through enzymolysis and fermentation pretreatments. Enzymes are catalytic proteins capable of purposefully shearing peptides owing to their high selectivity (Henzler-Wildman et al., 2007). Cellulase is a multi-enzyme complex that hydrolyzes plant cell walls, releases phenols and flavone, and increases the antioxidant activity of products (Liu et al., 2017). α -Amylase and glycosylase exert a synergistic effect and significantly increase the reducing sugar content in the product. Fermentation treatment retains the original nutrients of coarse cereals, and microorganisms degrade starch, protein, and other macromolecules, thereby increasing the amount of beneficial prebiotics in the human body (Poutanen et al., 2009). Microbial fermentation can produce esters, alcohols, and other flavoring substances that improve the product flavor (Smid & Kleerebezem, 2014). In addition, it can improve the antioxidant activity and degrade anti-nutrients and harmful substances (Duan et al., 2020).

PCA is a statistical method that is used for dimensional-reduction of the data to obtain maximum information of original variables. Factor analysis was performed to extract and simplify multiple indicators, and the product quality was compared in a study (Gao et al., 2013). Gao et al. (2018) used crisp yam tablets prepared by four drying methods as the research objects and conducted PCA on eight types of aroma components to finally obtain the optimal comprehensive product by using load diagram and the principal component score. Liu et al. (2016) used *pachyrhizus erosus* as the raw material and supplemented it with *capsicum frutescens* L. to conduct PCA of the flavor substances. The flavor substances added by different fermentation methods were analyzed, and the PCA extracted two PCs. Granato et al. (2018) discussed the application of PCA to explore the

correlation between bioactive and functional substances, and their study revealed that the correlation coefficient could be applied to appropriately examine the correlation between the content and biological activity of compounds. Ito et al. (2018) studied the functional chemicals and lipid antioxidant activities of 21 algae species from the Japanese coast. The correlation between the chemical substances and algae phylum was detected by PCA.

In the present study, we used purple sweet potato, soybean, peanut kernel, sesame seed, corn, millet, brown rice, quinoa, semen coicis, and highland barley that were subjected to enzymolysis (by cellulase, α -amylase, and glycosylase) and fermentation (by *Lactobacillus plantarum* and *Lactobacillus acidophilus*) technology to prepare the desired CCCP. The effects of pretreatments on the quality properties, and the microstructure of CCCP were then investigated.

2 | MATERIALS AND METHODS

2.1 | Materials and reagents

Purple sweet potato, soybean, peanut kernel, sesame seed, corn, millet, brown rice, quinoa, semen coicis, and highland barley were sourced from the market.

Cellulase (4×10^5 U/g) was purchased from Shanghai Ruiyong Biological Technology Co., Ltd. (Shanghai, China). α -amylase (4×10^3 U/g), glycosylase (1×10^5 U/g), and glucose were purchased from Dalian Meilun Company (Dalian, China), *Lactiplantibacillus plantarum* and *Lactobacillus acidophilus* were purchased from Shandong Zhongke Jiayi Biological Engineering Co., Ltd. (Shandong, China). Other chemicals used were of analytical reagent grade.

2.2 | Sample preparation and treatment

According to the appropriate intake, the formula of CCCP was determined using the linear programming method and

optimized using Plackett—Burman and Box—Behnken designs. The formula used was as follows: purple sweet potato 108.00 g, soybean 58.00 g, peanut kernel 57.00 g, sesame seed 9.78 g, corn 8.00 g, millet 7.70 g, brown rice 5.47 g, quinoa 4.50 g, semen coicis 4.00 g, and highland barley 3.00 g (Gao et al., 2022).

After a large number of preliminary experiments, enzymolysis and fermentation conditions were obtained as follows: In the enzymolysis group, for cellulase, the enzymolysis time was 110 min, the temperature was 55°C, and the enzymolysis addition amount was 0.75%. In addition, the multi-enzymes ratio (α -amylase: glycosylase) was 1:2, enzymolysis time and temperature were 130 min and 55°C, respectively, and the multi-enzymes addition amount was 0.75%. In the fermentation group, the inoculation ratio (*L. plantarum*: *L. acidophilus*) was 1:1, fermentation time and temperature were 7 h and 24°C, respectively, and the inoculation amount was 9%. In the joint group, CCCP was prepared first by enzymolysis and then by fermentation. For the blank group, no pretreatment was performed, with all other conditions remaining unchanged.

The 10 pretreatment raw materials were beaten with the colloid mill (SOT; Shenyang Liyuan Motor Co., Ltd., Liaoning, China) and treated with a high-pressure homogenizer at the homogenization pressure of 40 MPa for 2–5 min (Scientz-150; Ninbo Xinzhi Biotechnology Co., Ltd., Zhejiang, China). Then, CCCP was obtained using a laboratory-scale spray dryer (SD-1500; Shanghai Wodi Technology Co., Ltd., Shanghai, China) at the spray pressure of 0.20 MPa, the feed flow rate of 400 ml/h, inlet air temperature of 160°C, and the drying airflow rate of 45 m³/h.

2.3 | Antioxidative assay

2.3.1 | Preparation of extracts

Dried pretreatment samples (1 g) were extracted twice with 50 ml of 80% ethanol solution, followed by intermittent breaking with a homogenizer at 5000 rpm for 5 min. The supernatant was collected after ultrasonic extraction for 20 min and centrifuged at 5000 rpm for 15 min. Following twice extraction, the extracts were combined, and the volume was made up to 50 ml. The solution was stored at 4°C until use.

2.3.2 | DPPH radical scavenging activity

The sample extracts (0.1 ml) were collected in a 10-ml centrifuge tube, to which 2 ml of 0.2 mmol/L DPPH and 2.9 ml of anhydrous ethanol were added. The solution was

mixed evenly and placed in the dark for 30 min. Anhydrous ethanol was used as the blank control, and the absorbance value was measured at 517 nm. The DPPH• scavenging activity of the samples was calculated using formula (1) (Sahreen et al., 2010):

$$\text{DPPH} \cdot \text{scavenging activity} / \% = \left[1 - \frac{A_i - A_j}{A_c} \right] \times 100\% \quad (1)$$

where A^c is the absorbance value when anhydrous ethanol is used to replace the sample solution, A_j is the absorbance value when adding the sample and replacing DPPH with anhydrous ethanol, and A_i is the absorbance value when the sample and DPPH are added.

2.3.3 | ABTS radical scavenging activity

The ABTS solution (7 mmol/L) was evenly mixed with 2.45 mmol/L of potassium persulfate solution at the ratio of 1:1 and placed at room temperature in the dark for 14–16 h; the resulting solution was recorded as the ABTS mother solution. To prepare the ABTS working solution, the absorbance value of the ABTS mother solution was diluted to a wavelength of 734 nm was 0.72–1.20 with pH 7.4 with 0.20 mol/L phosphate-buffered saline.

Then, 1 ml of the sample extracts was added to 4 ml of the ABTS working solution and allowed to react for 6 min. Phosphate buffer was used as the blank control, and the absorbance value was measured at 734 nm. Distilled water served as the blank control group. The ABTS⁺ scavenging activity of the samples was calculated using formula (2) (Re et al., 1999):

$$\text{ABTS}^+ \text{scavenging activity} / \% = \frac{A_{C2} - A_{S2}}{A_{C2}} \times 100\% \quad (2)$$

where A_{C2} and A_{S2} are the absorption values of the blank control group and the sample group, respectively.

2.3.4 | OH radical scavenging activity

For this assay, 2 ml of 9 mmol/L H₂O₂, FeSO₄, and the sample extracts were added to a 15-ml colorimetric tube, uniformly mixed, and allowed to react at 25°C for 10 min. Then, 2 ml of 9 mmol/L salicylic acid was added to the mixture and allowed to react for 30 min. The absorbance value was measured at 510 nm, and the OH• scavenging activity of the samples was calculated using formula (3) (Wang et al., 2021):

$$\text{OH} \cdot \text{scavenging activity} / \% = \left[1 - \frac{A_1 - A_2}{A_0} \right] \times 100\% \quad (3)$$

where A_0 is the absorption value of 2 ml deionized water + 2 ml FeSO_4 + 2 ml H_2O_2 + 2 ml salicylic acid; A_1 is the absorbance value of 2 ml sample extract + 2 ml FeSO_4 + 2 ml H_2O_2 + 2 ml salicylic acid; and A_2 is the absorbance value of 2 ml sample extract + 6 ml deionized water.

2.3.5 | O_2 radical scavenging activity

Tris-HCl buffer solution (1.84 ml, pH = 8.1) was added to 0.4 ml of the extracts and allowed to react for 10 min in a water bath at 37°C, followed by the addition of 0.16 ml of the pyrogallol acid solution. After 4 min of rest, 0.5 ml of concentrated sulfuric acid was added to terminate the reaction. The absorbance value was measured at 325 nm, and the O_2^- scavenging activity of the samples was calculated using formula (4) (Li et al., 2018):

$$\text{O}_2^- \text{ scavenging activity} / \% = \frac{A_0 - A_1}{A_0} \times 100\% \quad (4)$$

where A_0 is the absorption value of distilled water and free radical, and A_1 is the absorbance value of the sample and free radical.

2.3.6 | Fe radical chelating capacity

The sample extract (1 ml) was taken in a tube, to which 2 ml of FeCl_2 and 2 ml of the ferrozine solution were added, mixed evenly, and allowed to react for 10 min. Then, the absorbance value of the solution was measured at 562 nm. The Fe^{2+} -chelating capacity of the samples was calculated using formula (5) (Xie et al., 2008):

$$\text{Fe}^{2+} \text{ chelating capacity} / \% = \left[1 - \frac{A_1}{A_0} \right] \times 100\% \quad (5)$$

where A_1 is the absorption value of the sample, and A_0 is the absorption value when the sample is replaced with distilled water.

2.4 | Functional components assay

2.4.1 | Anthocyanin content assay

The extracts were prepared using the method described in Section 2.3.1. Briefly, 2 ml of the extracts was made to a volume 50 ml separately with pH 1.0 buffer and pH 4.5 buffer and then heated in a 30°C-water bath for 60 min. The absorbance values were measured at 520 nm and 700 nm, respectively, whereas the anthocyanin content of the samples was calculated using formula (6) (Siddiq et al., 2018):

$$\text{Anthocyanin content} / (\text{mg}/100 \text{ g}) = \frac{A \times M \times v}{E \times m} \times 100 \quad (6)$$

where A is ($A_{520} - A_{700}$) pH 1.0 - ($A_{520} - A_{700}$) pH 4.5; M is the molar mass of centaurea-3-glucoside (449.2 g/mol); v is the extract volume (ml); E is the molar extinction coefficient of centaurea-3-glucoside [26 900 L/(mol·cm)]; and m is the sample mass (g).

2.4.2 | Flavone, soluble dietary fiber, reducing sugar, and protein content assay

The extracts were prepared using the method described in Section 2.3.1. Flavone content was determined using the aluminum nitrate colorimetric method.

Soluble dietary fiber content was determined according to the GB/T5009.88-2014 "Determination of dietary fiber in foods" (National Health & Family Planning Commission of the P.R.C., 2016).

The reducing sugar content was determined using the DNS method.

Protein content was determined according to the GB/T5009.5-2016 "Determination of protein in foods" (National Health & Family Planning Commission of the P.R.C. & State Food & Drug Administration, 2017a).

2.5 | Thermodynamic property assay

The samples were analyzed through differential scanning calorimetry (DSC). Briefly, 5 mg of the samples was taken in a DSC crucible, whereas an empty crucible was used as the blank control. The test conditions were: a temperature range of 20–200°C and a heating rate of 10°C/min. The onset gelatinization temperature T_0 , peak temperature T_p , termination temperature T_c , and enthalpy change ΔH of the samples were analyzed.

2.6 | Particle size assay

The particle size distribution of CCCP was tested with a laser particle size analyzer. Briefly, 2.5 mg of the samples was added to 10 ml of deionized water, and the solution was magnetically stirred for 60 min at 25°C.

2.7 | SEM assay

The microstructure of the samples was analyzed through SEM. The samples were fixed on a carrier plate and gilded by sputtering, after which the microstructure of the samples was observed under the SEM.

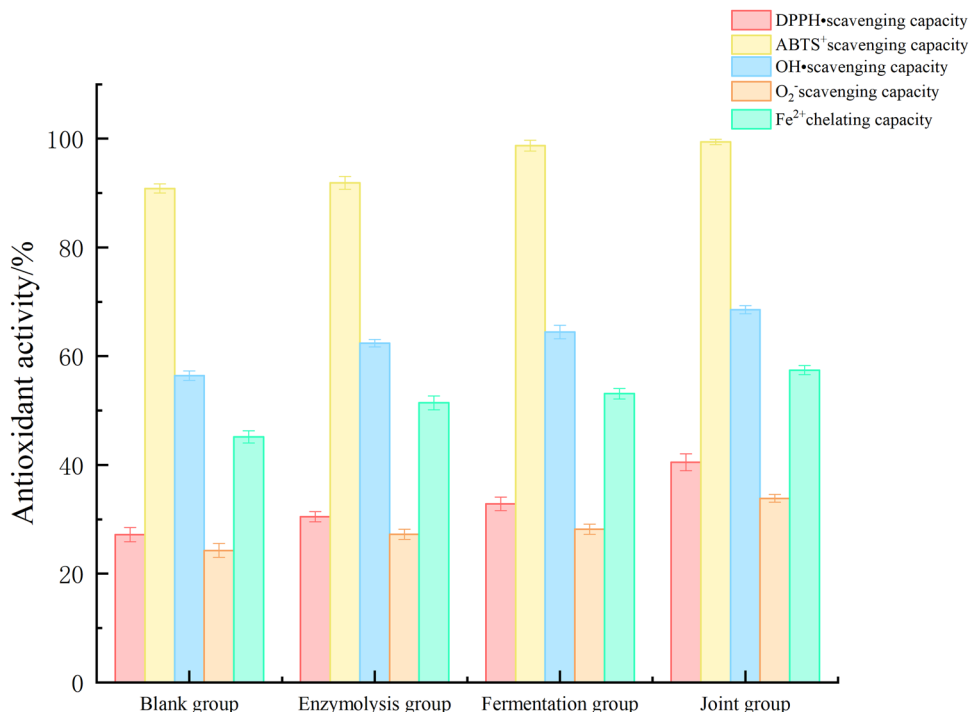


FIGURE 1 Effect of different treatment methods on the antioxidant activity of CCCP

2.8 | FTIR assay

The samples were tested by FTIR under the following test conditions: scanning wavenumber range, 400–4000 cm^{-1} ; resolution, 8 cm^{-1} ; and scanning times, 64 times.

2.9 | Microorganism detection

Microbial detection was performed according to the GB/T4789.1-2016 “National Standards for Food Safety General Provisions for Food Microbiology Inspection”(National Health & Family Planning Commission of the P.R.C. & State Food & Drug Administration, 2017b).

2.10 | Statistical analysis

Each treatment group was independently tested thrice. The experimental data was expressed as mean \pm standard deviation. Origin software was used for plotting, whereas SPSS software was used for data correlation analysis and PCA.

3 | RESULTS AND DISCUSSION

3.1 | Antioxidant activity analysis

The scavenging capacity of DPPH• and ABTS⁺ reflects the antioxidant capacity of the products (Malunga & Beta, 2015). As shown in Figure 1, the DPPH• scavenging capac-

ity of the enzymolysis group ($30.468\% \pm 0.949\%$), the fermentation group ($32.865\% \pm 1.244\%$), and the joint group ($40.490\% \pm 1.572\%$) increased by 12.10, 20.92, and 48.98%, respectively, compared with that of the blank group. The ABTS⁺ scavenging capacity of the three pretreatment groups was also improved, with the joint group having the highest capacity ($99.412\% \pm 0.515\%$). These results indicated that enzymolysis and fermentation could improve the scavenging capacity of DPPH• and ABTS⁺. DPPH• is an N-central free radical. The “free radical” released in the enzymolysis process donates its own electron to the lone electron of DPPH•, and DPPH• quenching by pairing improves the antioxidant activity of the enzymatic hydrolysate. In addition, phenolic compounds were positively correlated with DPPH• and ABTS⁺. Cellulase and multi-enzymes hydrolyzed the cell wall and aleurone layer, resulting in phenolic exposure, soluble dietary fiber outflow, and increased DPPH• and ABTS⁺ clearance (Wang et al., 2018). Dehydroxylase and phenolic acid decarboxylase produced during the fermentation process can weaken the ether bond between conjugated phenolic substances and cell wall and increase the content of free flavonoids and polyphenols, thereby increasing the antioxidant activity of DPPH• and ABTS⁺ (Muñoz et al., 2017).

OH• could cause biological membrane peroxidation, cancer, tumor, and other diseases (Zhang et al., 2009). O₂⁻ produced by an organism’s metabolism also induces mutations in proteins, nucleic acids, and polysaccharides and

TABLE 1 Functional components of coarse cereal compound powder (CCCP) with different treatment methods

	Anthocyanin /(mg/100 g)	Flavone /(mg/100 g)	Soluble dietary fiber /%	Reducing sugar/%	Protein/%
Blank group	0.443±0.003 ^b	0.391±0.021 ^c	5.190±0.901 ^d	17.688±1.506 ^b	35.700±0.347 ^a
Enzymolysis group	0.496±0.013 ^a	0.444±0.011 ^c	9.828±1.242 ^c	33.497±0.848 ^a	32.210±0.342 ^b
Fermentation group	0.203±0.004 ^c	0.815±0.028 ^b	12.784±0.962 ^b	10.777±0.232 ^c	12.941±0.442 ^d
Joint group	0.214±0.004 ^c	1.202±0.044 ^a	14.877±0.912 ^a	11.487±0.291 ^c	13.741±0.162 ^c

even necrosis. Therefore, reducing the OH• and O₂⁻ content in vivo is necessary. In addition, Fe²⁺ was considered the main component of haemoglobin and cytochrome, which played a positive role in the growth and development of the human body (Kasozzi et al., 2019). Figure 1 displays that the enzymolysis, fermentation, and joint groups all exhibited the increased OH• scavenging capacity, O₂⁻ scavenging capacity, and Fe²⁺ chelating capacity. Transition metal ions such as ferrous ions catalyze the reaction of O₂⁻ with H₂O₂ to produce more toxic OH• and OH⁻. However, the interaction between multi-enzymes and cellulase can open the fiber network structure of the molecule, and the increase in the specific surface area promotes the chelation of ferrous metal ions and then blocks the Fe²⁺ catalytic reaction. Therefore, it also has a strong ability to remove OH• (Wang et al., 2018). In addition, protease can be produced by fermentation. Histidine and methionine released by protease during hydrolysis contain active amino acids such as indolyl and imidazolyl, which play an important role in Fe²⁺ chelating capacity. The release of arginine and lysine exposes the -NH₂ group and increases the antioxidant activity.

3.2 | Functional component analysis

Anthocyanin is an excellent free radical scavenger and a lipid peroxidation inhibitor (Rivero-Pérez et al., 2008). As shown in Table 1, compared with that of the blank group, the anthocyanin content of the enzymolysis group had increased. This result may be attributed to anthocyanin release from the cells under moderate enzymolysis. Specifically, cellulase facilitated the enzymolysis of plant cell walls, which subsequently prompted anthocyanin outflow. The anthocyanin content of the fermentation group and the joint group decreased, which indicated that fermentation reduced the anthocyanin content. The decrease in the anthocyanin content caused by fermentation may be related to the bacterial metabolic activity, change in the sugar content, water mobility, and other factors. In addition, the decrease in the anthocyanin content may be attributed to the potential interaction such as absorption, degradation, and pH change of extracellular matrix between bacteria and anthocyanin (Sánchez-Velázquez et al., 2021). Flavonoids have strong antioxidant activities,

which prevent cardiovascular and cerebrovascular diseases (Siow & Mann, 2010). Because the chemical structure of flavonoids contains an o-diphenol group, a 2–3 double bond conjugated to a 4-carbonyl group and to the hydroxyl groups at positions 3 and 5 (Lee et al., 2004). Both enzymolysis and fermentation increased the flavonoid content, probably due to changes in the hydroxyl substitution of flavonoids due to multi-enzymes hydrolysis and microbial fermentation, making the electron spin density distribution of the flavanone semiquinone radical more uniform, and subsequently, increasing the flavonoid content. Moreover, fermentation destroyed the grain cell wall structure and released and induced bioactive substance synthesis. Amylase, chitinase, and other microbial enzymes produced by fermentation can decompose plant cell wall and starch, thereby promoting the release of flavonoids (Hur et al., 2014). The content of CCCP-soluble dietary fiber increased due to enzymolysis, which may be attributed to the cellulose decomposition of macromolecular compounds into small molecules. During fermentation, *L. plantarum* and *L. acidophilus* mutually generated more amylase and protease to promote the dissolution and synthesis of soluble dietary fiber, thereby increasing the soluble dietary fiber content. The content of reducing sugar in the enzymolysis group was higher than that in the blank group because α-amylase and glycosylase converted starch and other macromolecules into small molecules, thereby increasing the level of reducing sugar. During the fermentation process, microorganisms consume glucose and other substances to maintain normal growth and reproduction, reducing the reducing sugar content. The protein content changed less in the enzymolysis group; however, it was significantly lower in the fermentation and joint groups than in the blank group, probably because the protein was used by bacteria for growth and reproduction during the fermentation process.

3.3 | Correlational analysis between antioxidant activity and functional components

Correlation analyses were performed to analyze the scavenging capacity of DPPH•, ABTS⁺, OH•, and O₂⁻,

Fe^{2+} -chelating capacity, and the anthocyanin, flavone, soluble dietary fiber, reducing sugar, and protein contents of CCCP with different treatment methods. Table 2 shows the correlation between these 10 indicators. For example, the correlation coefficient between the DPPH•-scavenging capacity and protein content was -0.808 , which indicated that the correlation was highly significant and negative. The high protein content indicated that the amount of protein degraded through enzymolysis and fermentation and the amount of polypeptides with strong antioxidant properties were less, leading to the decrease in the DPPH•-scavenging capacity (Ikram et al., 2020). The correlation coefficient between the anthocyanin content and the reducing sugar content was 0.870 , which indicated that the correlation was significantly strong and positive. Anthocyanin synthesis is regulated by reducing sugar and other factors. Under certain conditions, the reducing sugar content affects the expression of anthocyanin biosynthesis-, transport-, and regulation-related genes and thus promotes the increase in the anthocyanin content. The correlation coefficient between the OH•-scavenging capacity and the Fe^{2+} -chelating capacity was 0.999 , indicating that the correlation was extremely strong and positive. The metal ion chelation rate is commonly used to evaluate the antioxidant capacity. The higher the chelation rate, the stronger is the potential antioxidant capacity. Therefore, the Fe^{2+} chelation capacity is positively correlated with the antioxidant capacity and OH•-scavenging capacity (Ma et al., 2013). The correlation coefficient between the flavone content and O_2^- -scavenging capacity was 0.947 , indicating that the correlation was extremely strong and positive. The structure of flavonoids often comprises phenolic, hydroxyl, methoxyl, methyl, isopentenyl, and other functional groups. O_2^- has a negative potential, and surplus electrons can supplement the ageing cells or blood cells to promote anti-oxidation and anti-ageing effects by eliminating free radicals (Yu et al., 2019). The correlation coefficient between the soluble dietary fiber content and the DPPH•-scavenging capacity was 0.915 , indicating that the correlation was extremely strong and positive. Enzymolysis and fermentation resulted in the degradation of macromolecular substances and generation of small molecular substances. The soluble dietary fiber content increased, the spaces between the molecules increased, and the polymerization degree decreased, promoting the release of phenolic substances and increasing the DPPH•-scavenging capacity (Fu et al., 2017). These results indicated that PCA can be used to analyze these variables.

3.4 | PCA between antioxidant activity and functional components

PCA is a multivariate statistical method used for transforming multiple variables into several important comprehensive variables for dimension reduction (Garazhian et al., 2020). Through orthogonal transformation, the original random variables related to their components [including the DPPH•-scavenging capacity (X_1), ABTS⁺-scavenging capacity (X_2), OH•-scavenging capacity (X_3), O_2^- -scavenging capacity (X_4), Fe^{2+} -chelating capacity (X_5), anthocyanin (X_6), flavone (X_7), soluble dietary fiber (X_8), reducing sugar (X_9), and protein (X_{10})] were transformed into the unrelated new random variables PC1 and PC2. At the algebraic level, the covariance matrix from X_1 to X_{10} was transformed into a diagonal row matrix. At the geometric level, the original coordinate system was replaced by a new orthogonal coordinate system, which pointed to the 10 most widely distributed orthogonal directions of the four groups of samples. Then the dimension reduction process was conducted for the multidimensional variable system, and the higher precision was converted to the lower dimensional variable system. By constructing the value function, the low-dimensional system was transformed into a one-dimensional system. According to Figure 2, two PCs were extracted using the PCA, and the cumulative variance contribution rate reached 97.014%. By dividing the value in the PC load matrix by the square root of the characteristic value corresponding to each PC, the PC coefficient matrix was obtained, and the linear relationship between PC and each index was determined according to the coefficient matrix. The two PCs were defined as PC1 and PC2. According to the principle of PCA, the linear combination of each PC was as follows:

$$\begin{aligned} \text{PC1} = & 0.326X_1 + 0.334X_2 + 0.325X_3 + 0.320X_4 \\ & + 0.322X_5 - 0.309X_6 + 0.336X_7 + 0.330X_8 \\ & - 0.214X_9 - 0.327X_{10} \end{aligned}$$

$$\begin{aligned} \text{PC2} = & 0.187X_1 - 0.170X_2 + 0.281X_3 + 0.257X_4 \\ & + 0.308X_5 + 0.388X_6 - 0.031X_7 + 0.188X_8 \\ & + 0.688X_9 + 0.190X_{10} \end{aligned}$$

As shown in Table 3, the characteristic value of PC1 was 8.471, and its variance contribution rate was 84.711%,

TABLE 2 Correlation of quality indices of CCCP with different treatment methods

	DPPH• scavenging capacity	ABTS ⁺ scavenging capacity	OH• scavenging capacity	O ₂ ⁻ scavenging capacity	Fe ²⁺ chelating capacity	Anthocyanin	Flavone	Soluble dietary fiber	Reducing sugar	Protein
DPPH• scavenging capacity	1.000									
ABTS ⁺ scavenging capacity	0.854**	1.000								
OH• scavenging capacity	0.946**	0.873**	1.000							
O ₂ ⁻ scavenging capacity	0.997**	0.820**	0.952**	1.000						
Fe ²⁺ chelating capacity	0.944**	0.857**	0.999**	0.952**	1.000					
Anthocyanin	-0.743**	-0.967**	-0.724**	-0.692**	-0.701**	1.000				
Flavone	0.970**	0.932**	0.901**	0.947**	0.892**	-0.876**	1.000			
Soluble dietary fiber	0.915**	0.920**	0.990**	0.912**	0.985**	-0.790**	0.899**	1.000		
Reducing sugar	-0.473	-0.725**	-0.337	-0.402	-0.309	0.870**	-0.670**	-0.406	1.000	
Protein	-0.808**	-0.996**	-0.853**	-0.773**	-0.836**	0.966**	-0.895**	-0.911**	0.713**	1.000

**indicates extremely significant correlation ($p < 0.01$).

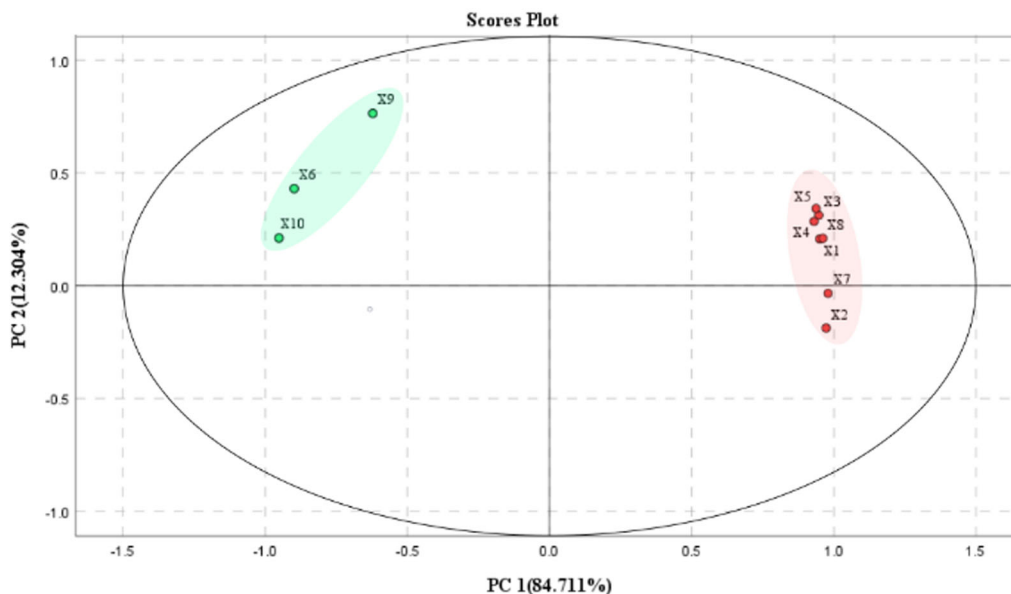


FIGURE 2 PCA of CCCP with different treatment methods

TABLE 3 The loading matrix of the two principal components (PCs) used in this study

Factor	PC1		PC2	
	Load	Eigenvector	Load	Eigenvector
DPPH• scavenging capacity	0.950	0.326	0.207	0.187
ABTS ⁺ scavenging capacity	0.973	0.334	-0.188	-0.170
OH• scavenging capacity	0.947	0.325	0.312	0.281
O ₂ ⁻ scavenging capacity	0.930	0.320	0.285	0.257
Fe ²⁺ chelating capacity	0.937	0.322	0.342	0.308
Anthocyanin	-0.898	-0.309	0.430	0.388
Flavone	0.979	0.336	-0.034	-0.031
Soluble dietary fiber	0.961	0.330	0.209	0.188
Reducing sugar	-0.622	-0.214	0.763	0.688
Protein	-0.952	-0.327	0.211	0.190
Eigenvalue	8.471		1.230	
Explained variance/%	84.711		12.304	

which mainly included the DPPH•-scavenging capacity, ABTS⁺-scavenging capacity, OH•-scavenging capacity, O₂⁻-scavenging capacity, Fe²⁺-chelating capacity, and the flavone and soluble dietary fiber contents. The characteristic value of PC2 was 1.230, whereas its variance contribution rate was 12.304%, which mainly included the anthocyanin, reducing sugar, and protein contents.

3.5 | Comprehensive evaluation of CCCP quality

The 10 factors were linear combined as a new comprehensive index, and the weighted sum of the two PCs was used to obtain the final evaluation value. The com-

prehensive evaluation model $PC = 0.847PC1 + 0.123PC2$ was established based on the variance contribution rate of the characteristic values corresponding to each PC. The comprehensive score was then calculated (comprehensive score = $\sum PC * \text{variance contribution rate}$, where variance contribution rate = $\frac{PC \text{ variance contribution value}}{\text{sum of PC variance contribution rate}}$). According to the sample score, the ranking of the four groups was determined. The results indicated that the fermentation group and the joint group ranked top in PC1, indicating that the scavenging capacities of DPPH•, ABTS⁺, OH•, O₂⁻, Fe²⁺-chelating capacity, and contents of flavone and soluble dietary fiber of these two groups were relatively high, among which the PC1 of the joint group was up to 3.34. In PC2, the enzymolysis group was superior to the other three

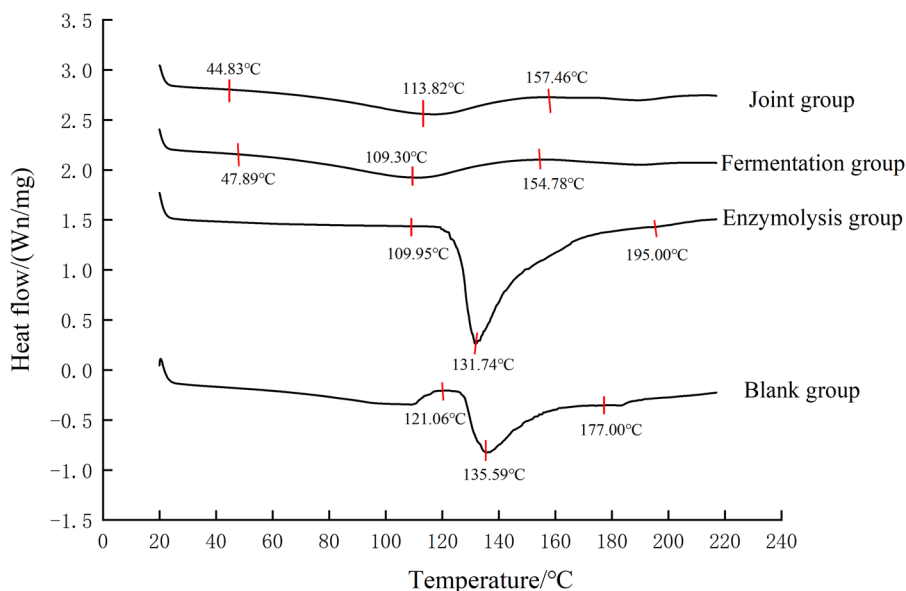


FIGURE 3 DSC gelatinization curves of CCCP

groups, indicating that the sample treated by enzymolysis had high contents of anthocyanin, reducing sugar, and protein. Overall, the four samples were ranked as follows: joint group > fermentation group > enzymolysis group > blank group. The results showed that the antioxidant activity and the content of functional components were improved by enzymolysis, fermentation, and joint treatments.

3.6 | Thermodynamic property analysis

Figure 3 displays the DSC gelatinization curves of the four groups of samples. The thermal property curves of all samples were unimodal due to amylopectin gelation. In the blank group, T_0 was $121.06 \pm 0.06^\circ\text{C}$, T_P was $135.59 \pm 0.06^\circ\text{C}$, and ΔH was $58.21 \pm 0.04 \text{ J/g}$. In the enzymolysis group, T_0 was $109.95 \pm 0.04^\circ\text{C}$, T_P was $131.74 \pm 0.05^\circ\text{C}$, and ΔH was $149.60 \pm 0.04 \text{ J/g}$. Compared with that in the blank group, T_0 decreased in the enzymolysis group because α -amylase, glycosylase, and cellulase hydrolyzed amylose, which was not easily gelatinized or dissolved into dextrin and other substances dominated by short chains. Consequently, the connection between amylose and amylopectin was weakened, making the starch grains more absorbent and gelatinized, thus decreasing T_0 . ΔH significantly increased, possibly because the number of short-chain molecules increased in the system after enzymolysis of CCCP. Owing to the formation of the double helix structure, an ordered crystal structure was formed, increasing the amount of heat required for the destruction of the structure during gelatinization, thereby significantly increasing ΔH . The T_0 of the fermentation group was lower than that of the blank group, indicating that CCCP treated by fermentation was easier to gelatinize.

The decrease in the gelatinization temperature was due to the destruction of the amorphous area of starch particles by acids and enzymes generated through microbial metabolism in the fermentation process (Hagenimana et al., 2005), which enhanced the water-binding ability of starch particles and rendered them easier to gelatinize. In addition, fermentation reduced the protein content, which weakened the complexation ability with starch, thereby reducing the gelatinization temperature. In the fermentation group, T_P was $109.30 \pm 0.03^\circ\text{C}$, and ΔH was $59.62 \pm 0.04 \text{ J/g}$. The ΔH increase may be attributed to the acids and enzymes produced by fermentation, which reduced the amorphous area of starch particles, whereas the crystallization area increased, which in turn increased the ΔH . In the joint group, T_P was $113.82 \pm 0.07^\circ\text{C}$, ΔH was $61.21 \pm 0.10 \text{ J/g}$, and T_0 was much lower than that in the blank group.

3.7 | Particle size analysis

Figure 4 depicts the particle size distribution of CCCP with different treatment methods. After enzymolysis, fermentation, and joint treatment, the particle size distribution of the samples changed from a single peak to a double peak. The average particle size of CCCP decreased from 26.4 to 8.95 μm , whereas the specific surface area increased from 216.3 to 638.4 m^2/kg by enzymolysis with cellulase, α -amylase, and glycosylase. This result can be attributed to the degradation of starch and cellulose into small molecules due to hydrolysis by multi-enzymes, which reduced the particle size. The average particle size of CCCP decreased from 26.4 to 8.12 μm , whereas the specific surface area increased from 216.3 to 703.6 m^2/kg .

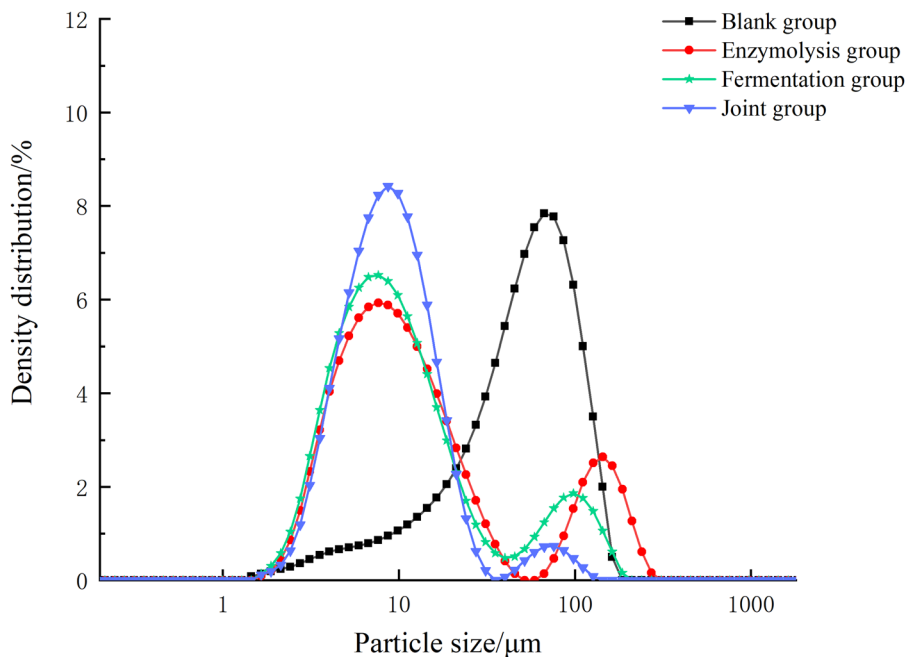


FIGURE 4 Particle size distribution of CCCP for different treatment methods

after fermentation with *L. plantarum* and *L. acidophilus*. Because fermentation can uniformly destroy CCCP particles and effectively degrade protein molecules and convert them into peptides, the average particle size of CCCP particles was reduced (Aguirre et al., 2014). The results suggested that the average particle size increased from 26.4 to 7.93 μm , whereas the specific surface area increased from 216.3 to 721.0 m^2/kg by joint treatment. The average particle size was lower in the joint group than that in the enzymolysis or fermentation alone treatment groups, because enzymolysis and fermentation have a synergistic effect, further reducing the particle size and improving hydration and powder properties. The decrease in the average particle size occurred in parallel with an increase in the specific surface area of the sample, and the surface cohesion and adsorption force enhanced, which proved beneficial to improve the fluidity and stability of the product.

3.8 | SEM analysis

As shown in Figure 5, after the hydrolysis of CCCP by multi-enzymes, the elliptic morphology of the original molecular particles changed into an irregular shape with a rough surface. The enzymes destroyed the combination of starch and protein to a certain extent because the granules, after enzymatic hydrolysis, rearrange amylose and amylopectin to form microcrystalline bundles, resulting in the formation of a new microstructure, which makes the starch harder and increases its crystal density. In the blank group, starch and protein were bound

more tightly. The disulphide bond between the proteins causes the protein to wrap in the surface of starch to form a reticular structure that hinders the exposure and release of starch and exerts a certain hindering effect on the swelling of starch. In this case, a continual and clear bundle gluten network structure, embedded by starch particles, was observed. After fermentation, CCCP molecular particles became smaller. The complete structure of CCCP was destroyed by the growth and decomposition of *L. plantarum* and *L. acidophilus*, and the active substances were easier to extract, which improved the antioxidant activity of CCCP. CCCP treated with the joint treatment displayed a more serious molecular particle breakage effect than those by enzymolysis or fermentation treatment alone, indicating that enzymolysis and fermentation exert a synergistic effect on starch and protein release, thereby enhancing the water-holding capacity and the antioxidant activity.

3.9 | FTIR analysis

Figure 6 displays the CCCP infrared spectrograph of different treatments. As shown in the figure, the absorption band at $1000\text{--}1125\text{ cm}^{-1}$ reflects the C—O stretching vibration of alcohols and phenols. Compared with the blank group, the absorption intensity of the characteristic peak increased in this range in the enzymolysis group. After fermentation treatment, the intensity of the characteristic peaks at $3100\text{--}3500\text{ cm}^{-1}$ and $2843\text{--}3000\text{ cm}^{-1}$ weakened, which can be attributed to NH stretching vibration of amide and the C—H stretching vibration of alkane, respectively. The characteristic peak of proteins weakened or

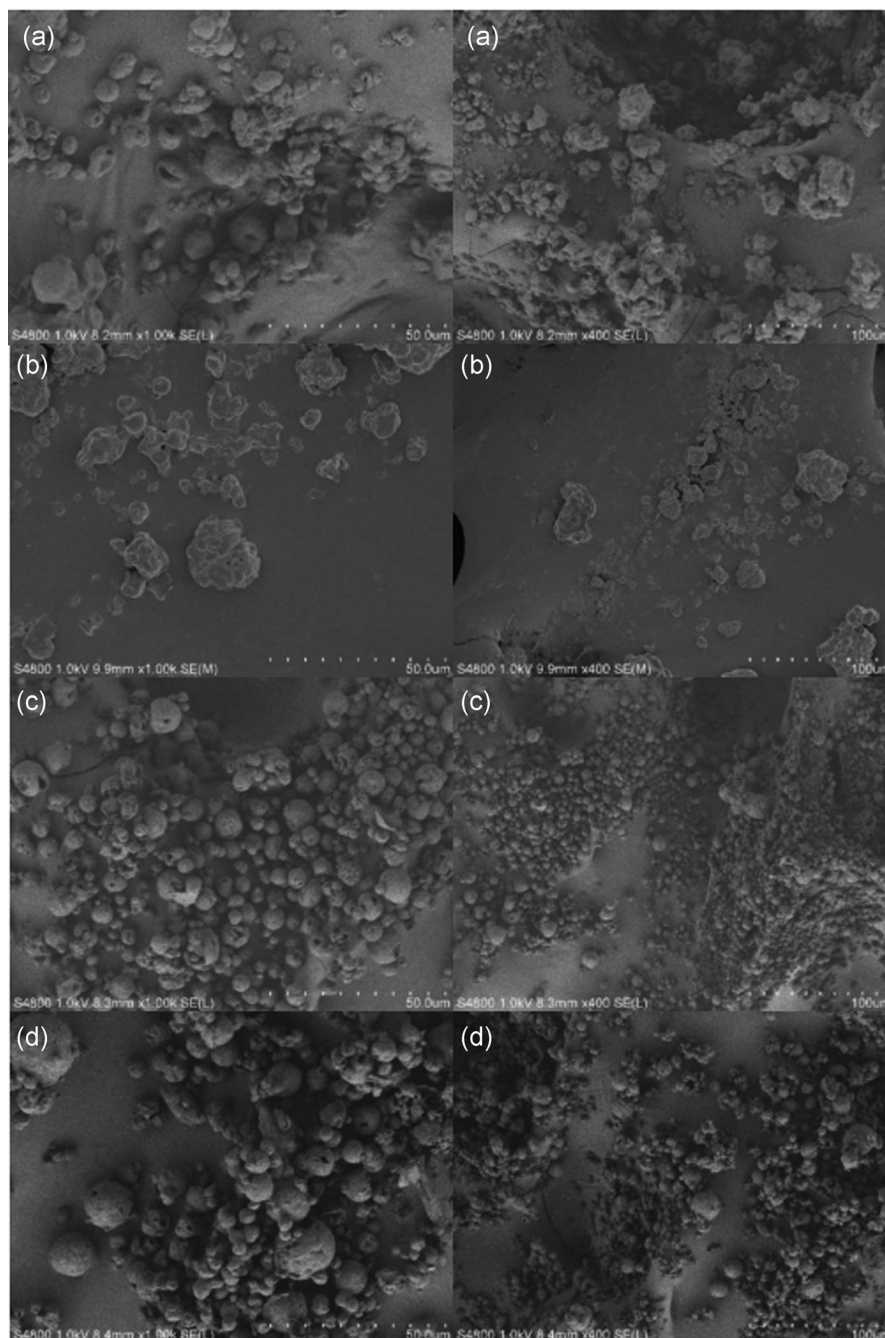


FIGURE 5 SEM images of different treatments. A is 1000 times of amplification in the blank group; a is 400 times amplification in the blank group; B is 1000 times amplification in the enzymolysis group; b is 400 times amplification in the enzymolysis group; C is 1000 times amplification in the fermentation group; c is 400 times amplification in the fermentation group; D is 1000 times amplification in the joint group; and d is 400 times amplification in the joint group

disappeared in the range of $1600\text{--}1700\text{ cm}^{-1}$, which was mainly related to amide I band $\text{C}=\text{O}$ stretching vibration (Byler & Susi, 1986). The spectral band of the fermentation group at 1122 cm^{-1} can be attributed to the two main vibration modes: $\text{C}-\text{O}$ stretching and $\text{C}-\text{O}-\text{H}$ bending (Kizil et al., 2002). After fermentation, the sample exhibited a significant peak at $615\text{--}645\text{ cm}^{-1}$, which can be attributed to the out-of-plane bending vibrations of alkynes CH . The

characteristic peak of the joint group was the same as that of the fermentation group, albeit the intensity of the characteristic peak was increased.

The secondary protein structures included α -helix ($1650\text{--}1659\text{ cm}^{-1}$), β -sheet ($1610\text{--}1639\text{ cm}^{-1}$), β -turn ($1660\text{--}1700\text{ cm}^{-1}$), and random coil ($1640\text{--}1649\text{ cm}^{-1}$) (Ai et al., 2019). Their relative contents in the secondary structure of the blank group were as follows: α -helix

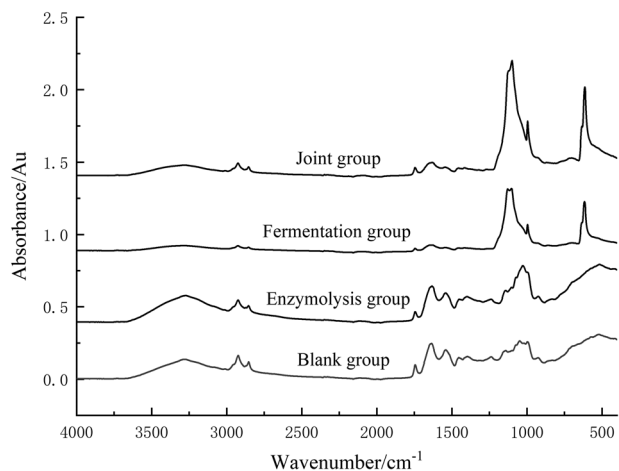


FIGURE 6 Infrared spectrum analysis of CCCP with different treatment methods

content, 16.80%; β -sheet content, 39.29%; β -turn content, 25.01%; and random coil content, 18.90%. Compared with those of the blank group, the contents of β -sheet (40.25%) and β -turn (25.22%) in the secondary structure of the enzymolysis group increased, whereas those of α -helix (16.46%) and random coil (18.07%) decreased. Thus, the α -helix structure was disrupted by enzymolysis, and the protein was decomposed into small peptides, which can be easily absorbed by the human body. Enzymolysis uncoiled the protein helix structure (Qian et al., 2016), and α -helix and random coil were converted into β -sheet and β -turn to a certain extent. In the fermentation group, α -helix disappeared, the β -sheet content (32.97%) decreased, and the β -turn (25.44%) and random coil contents (41.60%) increased. This effect can be attributed to the long fermentation time that disrupted the hydrogen bond connecting the α -helix, which was transformed into an irregular structure, and the reaction depolymerized and rearranged. In the joint group, the α -helix content (40.41%) increased, β -sheet (35.03%) and β -turn contents (24.56%) decreased, and random coil disappeared. Because α -helix is a relatively stable and ordered protein secondary structure, a significant increase in its content in the joint group indicated that the sample had strong stability (Choi & Ma, 2007). The decrease in the β -sheet content led to the exposure of the hydrophobic protein group. Hydrophobic amino acids could promote the interaction between hydrophobic polyunsaturated fatty acids and antioxidant peptides and inhibit lipid peroxidation, thereby improving the antioxidant activity of the samples (Mendis et al., 2005).

3.10 | Microorganism detection analysis

The total number of bacteria $\leq 1\ 000$ CFU/g, *Escherichia coli*, *Salmonella*, and *Staphylococcus aureus* were not enu-

merated in the four groups, so products are in line with national standards.

4 | CONCLUSION

Enzymolysis increased the contents of anthocyanin, flavone, soluble dietary fiber, and reducing sugar in CCCP. Fermentation and joint treatment methods produced significant effects on the antioxidant activity of CCCP. According to the established PCA model, the 10 indicators were correlated, and the cumulative contribution rate of the two PCs extracted from the PCA results reached 97.01%.

After enzymolysis and fermentation, the sensory quality of CCCP was improved, the T_0 decreased, the particle size decreased, and the specific surface area increased. Cell integrity in the enzymolysis group and fermentation group was damaged to varying degrees compared with that in the blank group, and the range and intensity of absorption peak were also changed to different degrees. SEM revealed that the molecular particles under different treatment groups were smaller and that the functional components such as flavonoids, soluble dietary fiber, alcohols, and esters were dispersed, which increased the antioxidant capacity. The aromatic alcohols and esters also enhanced the sensory quality. SEM confirmed the small size of the particles. SEM revealed that the state of the molecules transformed from compact to state, indicating that the links between amylose and amylopectin or other valence bonds were weakened or broken. This led to the easy gelatinization of particles, consistent with DSC results. The changes in the molecular structure also confirmed the results of secondary structure changes in FTIR.

The nutrient composition and bioavailability of coarse cereals can be greatly improved through enzymolysis and fermentation. In addition, exploring the antioxidant activity and functional components of CCCP with different treatment methods and analysing their microstructure can promote rational development and utilization of coarse cereal resources.

ACKNOWLEDGMENTS

This study was financially sponsored by the Special Fund of Liaoning Provincial Universities. Fundamental Scientific Research Projects(number LJKZ0998).

AUTHOR CONTRIBUTIONS

Conceptualization, L.G. and Y.C.; methodology, L.G.; software, Y.C. and L.C.; validation, L.G.; formal analysis, Y.C. and L.C.; investigation, Y.C.; resources, Y.C. and Z.G.X.; data curation, L.C.; writing—original draft preparation,

Y.C.; writing—review and editing, L.G.; visualization, L.C.; supervision, Z.G.X.; project administration, L.G.; funding acquisition, L.G. All authors have read and agreed to the published version of the manuscript.

CONFLICTS OF INTEREST

The authors declare no conflict of interest.

ORCID

Yue Chen  <https://orcid.org/0000-0002-9586-8042>

Lu Gao  <https://orcid.org/0000-0003-0615-9947>

REFERENCES

- Aguirre, L., Hebert, E. M., Garro, M. S., & De Giori, G. S. (2014). Proteolytic activity of *Lactobacillus* strains on soybean proteins. *LWT-Food Science and Technology*, *59*(2), 780–785. <https://doi.org/10.1016/j.lwt.2014.06.061>
- Ai, M., Tang, T., Zhou, L., Ling, Z., Guo, S., & Jiang, A. (2019). Effects of different proteases on the emulsifying capacity, rheological and structure characteristics of preserved egg white hydrolysates. *Food Hydrocolloids*, *87*, 933–942. <https://doi.org/10.1016/j.foodhyd.2018.09.023>
- Byler, D. M., & Susi, H. (1986). Examination of the secondary structure of proteins by deconvolved FTIR spectra. *Biopolymers: Original Research on Biomolecules*, *25*(3), 469–487. <https://doi.org/10.1002/bip.360250307>
- Choi, S. M., & Ma, C. Y. (2007). Structural characterization of globulin from common buckwheat (*Fagopyrum esculentum* Moench) using circular dichroism and Raman spectroscopy. *Food Chemistry*, *102*(1), 150–160.
- Duan, X., Duan, S., Wang, Q., Ji, R., Cao, Y., & Miao, J. (2020). Effects of the natural antimicrobial substance from *Lactobacillus paracasei* FX-6 on shelf life and microbial composition in chicken breast during refrigerated storage. *Food Control*, *109*, 106906.
- Fu, X., Wu, W., Wu, X., & Wang, X. (2017). Effects of rice bran storage time on the antioxidant activity of rice bran soluble dietary fiber. *China Oils and Fats*, *42*(8), 32–36. CNKI:SUN:SSPJ.0.2019-10-043.
- Gao, B., Lu, Y., Sheng, Y., Chen, P., & Yu, L. (2013). Differentiating organic and conventional sage by chromatographic and mass spectrometry flow injection fingerprints combined with principal component analysis. *Journal of Agricultural and Food Chemistry*, *61*(12), 2957–2963.
- Gao, L., Chen, Y., Wu, C., & Wang, L. (2022). The invention relates to a meal substitute powder for purple sweet potato and a preparation method thereof (*Liaoning, China Patent No. CN113974104A*). Shenyang Normal University. <https://cprs.patentstar.com.cn/Search/Detail?ANE=9GFE2CAA9GED5AEA9EEA7ECA9IFH9DCC7DDA9DGE9FDE9EEB>
- Gao, Q., Zhang, J., Chen, J., Liu, C., Liu, C., & Xue, Y. (2018). Comprehensive evaluation of the effect of four drying methods on the aroma quality of Chinese Yam chips based on principal component analysis. *Food Science*, *39*(20), 175–181.
- Garazhian, M., Gharaghani, A., & Eshghi, S. (2020). Genetic diversity and inter-relationships of fruit bio-chemicals and antioxidant activity in Iranian wild blackberry species. *Scientific Reports*, *10*(1), 1–13.
- Granato, D., Santos, J. S., Escher, G. B., Ferreira, B. L., & Maggio, R. M. (2018). Use of principal component analysis (PCA) and hierarchical cluster analysis (HCA) for multivariate association between bioactive compounds and functional properties in foods: A critical perspective. *Trends in Food Science & Technology*, *72*, 83–90.
- Hagenimana, A., Pu, P., & Ding, X. (2005). Study on thermal and rheological properties of native rice starches and their corresponding mixtures. *Food Research International*, *38*(3), 257–266.
- Henzler-Wildman, K. A., Lei, M., Thai, V., Kerns, S. J., Karplus, M., & Kern, D. (2007). A hierarchy of timescales in protein dynamics is linked to enzyme catalysis. *Nature*, *450*(7171), 913–916.
- Hur, S. J., Lee, S. Y., Kim, Y. C., Choi, I., & Kim, G. B. (2014). Effect of fermentation on the antioxidant activity in plant-based foods. *Food Chemistry*, *160*, 346–356. <https://doi.org/10.1016/j.foodchem.2014.03.112>
- Ikram, S., Zhang, H., Ahmed, M. S., & Wang, J. (2020). Ultrasonic pretreatment improved the antioxidant potential of enzymatic protein hydrolysates from highland barley brewer's spent grain (BSG). *Journal of Food Science*, *85*(4), 1045–1059. <https://doi.org/10.1111/1750-3841.15063>
- Ito, M., Koba, K., Hikihara, R., Ishimaru, M., Shibata, T., Hatate, H., & Tanaka, R. (2018). Analysis of functional components and radical scavenging activity of 21 algae species collected from the Japanese coast. *Food Chemistry*, *255*, 147–156.
- Kasoz, N., Tandlich, R., Fick, M., Kaiser, H., & Wilhelmi, B. (2019). Iron supplementation and management in aquaponic systems: A review. *Aquaculture Reports*, *15*, 100221.
- Kizil, R., Irudayaraj, J., & Seetharaman, K. (2002). Characterization of irradiated starches by using FT-Raman and FTIR spectroscopy. *Journal of Agricultural and Food Chemistry*, *50*(14), 3912–3918.
- Lee, J., Koo, N., & Min, D. B. (2004). Reactive oxygen species, aging, and antioxidative nutraceuticals. *Comprehensive Reviews in Food Science and Food Safety*, *3*(1), 21–33. <https://doi.org/10.1111/j.1541-4337.2004.tb00058.x>
- Li, Y., Zhu, C., Zhai, X., Zhang, Y., Duan, Z., & Sun, J. (2018). Optimization of enzyme assisted extraction of polysaccharides from pomegranate peel by response surface methodology and their anti-oxidant potential. *Chinese Herbal Medicines*, *10*(4), 416–423.
- Liu, J., Bao, C., Chang, W., Ma, Q., & Sun, L. (2016). Nutrition analysis of *Pachyrhizus erosus* pickles by different fermentation process and principal component analysis of the flavor compounds. *Food and Fermentation Industries*, *42*(11), 212–218.
- Liu, W., Brennan, M. A., Serventi, L., & Brennan, C. S. (2017). Effect of cellulase, xylanase and α -amylase combinations on the rheological properties of Chinese steamed bread dough enriched in wheat bran. *Food Chemistry*, *234*, 93–102.
- Ma, T., Tian, C., Luo, J., Zhou, R., Sun, X., & Ma, J. (2013). Influence of technical processing units on polyphenols and antioxidant capacity of carrot (*Daucus carrot* L.) juice. *Food Chemistry*, *141*(3), 1637–1644. <https://doi.org/10.1016/j.foodchem.2013.04.121>
- Malunga, L. N., & Beta, T. (2015). Antioxidant capacity of arabinoxylan oligosaccharide fractions prepared from wheat aleurone using *Trichoderma viride* or *Neocallimastix patriciarum* xylanase. *Food Chemistry*, *167*, 311–319.
- Mendis, E., Rajapakse, N., & Kim, S. K. (2005). Antioxidant properties of a radical-scavenging peptide purified from enzymatically prepared fish skin gelatin hydrolysate. *Journal of Agricultural and Food Chemistry*, *53*(3), 581–587.
- Muñoz, R., De Las Rivas, B., De Felipe, F. L., Reverón, I., Santamaría, L., Esteban-Torres, M., Curiel, J., Rodríguez, H., & Landete,

- J. (2017). Biotransformation of phenolics by *Lactobacillus plantarum* in fermented foods. In Frias J., Martinez-Villaluenga C., & Peñas E. (Eds.), *Fermented foods in health and disease prevention* (pp. 63–83). Elsevier. <https://doi.org/10.1016/B978-0-12-802309-9.00004-2>
- National Health and Family Planning Commission of the P.R.C. (2016). Determination of dietary fibre in foods (GB/T5009.88-2014). China Standards Press. <https://max.book118.com/html/2018/1213/6000225050001235.shtm>
- National Health and Family Planning Commission of the P.R.C., & State Food and Drug Administration. (2017a). Determination of protein in foods (GB/T5009.5-2016). China Standards Press. <https://max.book118.com/html/2019/0310/6123042032002014.shtm>
- National Health and Family Planning Commission of the P.R.C., & State Food and Drug Administration. (2017b). National Standards for Food Safety General Provisions for Food Microbiology Inspection (GB/T4789.1-2016). China Standards Press. <https://max.book118.com/html/2019/0421/6235011011002024.shtm>
- Poutanen, K., Flander, L., & Katina, K. (2009). Sourdough and cereal fermentation in a nutritional perspective. *Food Microbiology*, 26(7), 693–699.
- Qian, J., Ma, L., Wang, L., & Jiang, W. (2016). Effect of pulsed electric field on structural properties of protein in solid state. *LWT-Food Science and Technology*, 74, 331–337.
- Re, R., Pellegrini, N., Proteggente, A., Pannala, A., Yang, M., & Rice-Evans, C. (1999). Antioxidant activity applying an improved ABTS radical cation decolorization assay. *Free Radical Biology and Medicine*, 26(9–10), 1231–1237.
- Rivero-Pérez, M., Muniz, P., & González-Sanjosé, M. (2008). Contribution of anthocyanin fraction to the antioxidant properties of wine. *Food and Chemical Toxicology*, 46(8), 2815–2822.
- Sahreem, S., Khan, M. R., & Khan, R. A. (2010). Evaluation of antioxidant activities of various solvent extracts of *Carissa opaca* fruits. *Food Chemistry*, 122(4), 1205–1211.
- Sánchez-Velázquez, O. A., Cuevas-Rodríguez, E.-O., Reyes-Moreno, C., Ríos-Iribe, É. Y., Hernández-Álvarez, A. J., León-López, L., & Milán-Carrillo, J. (2021). Profiling modifications in physicochemical, chemical and antioxidant properties of wild blackberry (*Rubus* sp.) during fermentation with EC 1118 yeast. *Journal of Food Science and Technology*, 58(12), 4654–4665. <https://doi.org/10.1007/s13197-020-04953-x>
- Siddiq, M., Dolan, K. D., Perkins-Veazie, P., & Collins, J. K. (2018). Effect of pectinolytic and cellulolytic enzymes on the physical, chemical, and antioxidant properties of blueberry (*Vaccinium corymbosum* L.) juice. *LWT*, 92, 127–132.
- Siow, R. C., & Mann, G. E. (2010). Dietary isoflavones and vascular protection: Activation of cellular antioxidant defenses by SERMs or hormesis? *Molecular Aspects of Medicine*, 31(6), 468–477.
- Smid, E., & Kleerebezem, M. (2014). Production of aroma compounds in lactic fermentations. *Annual Review of Food Science and Technology*, 5, 313–326.
- Wang, L., Luo, Y., Wu, Y., Liu, Y., & Wu, Z. (2018). Fermentation and complex enzyme hydrolysis for improving the total soluble phenolic contents, flavonoid aglycones contents and bio-activities of guava leaves tea. *Food Chemistry*, 264, 189–198. <https://doi.org/10.1016/j.foodchem.2018.05.035>
- Wang, Z., Liu, X., Bao, Y., Wang, X., Zhai, J., Zhan, X., & Zhang, H. (2021). Characterization and anti-inflammation of a polysaccharide produced by *Chaetomium globosum* CGMCC 6882 on LPS-induced RAW 264.7 cells. *Carbohydrate Polymers*, 251, 117129.
- Xie, Z., Huang, J., Xu, X., & Jin, Z. (2008). Antioxidant activity of peptides isolated from alfalfa leaf protein hydrolysate. *Food Chemistry*, 111(2), 370–376.
- Yu, Z., Xiao, Y., Shuang, Q., Xia, Y., & Zhang, F. (2019). Optimization of flavonoid extraction process and functional properties in Qingpiaoling tea. *Food Science and Technology*, 44(10), 235–240. <https://doi.org/10.13684/j.cnki.spkj.2019.10.040>
- Zhang, J., Zhang, H., Wang, L., Guo, X., Wang, X., & Yao, H. (2009). Antioxidant activities of the rice endosperm protein hydrolysate: Identification of the active peptide. *European Food Research and Technology*, 229(4), 709–719.

How to cite this article: Chen, Y., Chen, L., Xiao, Z., & Gao, L. (2022). Effects of enzymolysis and fermentation on the antioxidant activity and functional components of a coarse cereal compound powder based on principal component analysis and microstructure study. *Journal of Food Science*, 87, 3573–3587. <https://doi.org/10.1111/1750-3841.16217>